PHYSICAL REVIEW B **79**, 241308(R) (2009)

Large anisotropic adatom kinetics on nonpolar GaN surfaces: Consequences for surface morphologies and nanowire growth

Liverios Lymperakis* and Jörg Neugebauer

Department of Computational Materials Design, Max-Planck-Institut für Eisenforschung, Max-Planck-Str. 1, 40237 Düsseldorf, Germany

(Received 7 April 2009; revised manuscript received 15 May 2009; published 12 June 2009)

The diffusion barriers of Ga and N adatoms on the nonpolar *a*- and *m*-plane surfaces have been studied employing density-functional theory calculations. Our calculations reveal a strong in-plane anisotropy of the diffusion barriers for both surfaces: for the *a*-plane surface larger diffusion lengths parallel to the *c* axis are observed. For the *m*-plane surface the in-plane anisotropy is reversed, and significantly smaller barriers are found for diffusion normal to the [0001] direction. These results are consistent with the experimentally observed in plane growth anisotropy of the nonpolar GaN surfaces. Moreover, they indicate that the large aspect ratio achieved for *c*-axial GaN nanowires is not a consequence of a strong anisotropy in the adatom mobilities but is rather related to surface thermodynamics and nucleation.

DOI: 10.1103/PhysRevB.79.241308 PACS number(s): 61.46.Km, 68.35.Fx, 81.05.Ea, 71.15.Nc

GaN and related III-nitride-based semiconductors are materials widely used in the optoelectronics industry for short-wavelength photonic applications as well as for high-frequency high power devices. The majority of the devices are traditionally grown on the *c* plane of the wurtzitic structure. However, in order to avoid the built in spontaneous polarization fields associated with the polar *c* axis, the growth of nonpolar *a*-$(11\bar{2}0)$ and *m*-$(1\bar{1}00)$ plane surfaces has attracted considerable interest over the recent years.[1] A characteristic feature in the growth morphology of nonpolar GaN surfaces is a strong in-plane anisotropy: atomic force microscopy images reveal elongated stripes along the [0001] ($[11\bar{2}0]$) direction on the $(11\bar{2}0)$ $[(1\bar{1}00)]$ surfaces.[2–7] The anisotropic in-plane growth character of the nonpolar GaN surfaces has been attributed (i) to largely different adatom sticking coefficients at the various low index step edges,[2] (ii) to replicating the substrate morphology onto the film surface, and (iii) to the presence of stacking faults.[8] A detailed study on the adatom kinetics on the nonpolar GaN surfaces which would provide a deeper understanding of the above issues is lacking. Such a study would be also desirable to better understand and optimize the growth of modern one-dimensional nanostructures. An example are GaN-based nanowires (NWs) which have recently emerged as potential candidates for nanodevice applications.[9,10] The majority of the reported GaN NWs have their axial direction along the *c* axis, while the facets are assumed to consist of nonpolar surfaces.

Theoretical studies on the properties and growth of the nonpolar GaN surfaces are sparse and focus mainly on the atomic and electronic structure and the thermodynamics of those surfaces.[11–14] Therefore, in this Rapid Communication we present first-principles calculations on the adatom kinetics on both nonpolar GaN surfaces. Our calculations are based on density-functional theory using the generalized gradient approximation and the projector augmented wave approach.[15,16] The calculated lattice parameters are $a=3.248$ Å, $c/a=1.629$, and $u=0.377$. The surfaces are modeled by a slab geometry consisting of six GaN double layers and a vacuum region of 10 Å. Equivalent $8\times4\times1$ and $4\times4\times1$ Monkhorst-Pack meshes are used for the 1×1 *m* and *a* surface unit cells, respectively. The bottom side of the slab is passivated by partially charged pseudohydrogen atoms. The atoms in the top three layers have been allowed to fully relax until the forces are smaller than 1 meV/Å. The potential-energy surface (PES) is calculated by fixing the adatom laterally at various positions and allowing vertical relaxation. For calculating the adatom adsorption energies 2×2 surface unit cells are used for both nonpolar surfaces. Convergence with respect to cut-off energy, *k*-point sampling, supercell size, slab, and vacuum thickness has been explicitly checked and provides an accuracy in binding energies and energy barriers of better than 5 meV.

Using this approach we have studied the kinetics of a Ga adatom on the *m*-plane surface. We use 18 inequivalent lateral positions to sample the 1×1 surface unit cell. The corresponding energies are used to construct the potential-energy surface based on an expansion in symmetrized plane waves and employ a singular value decomposition to obtain the expansion coefficients. The resulting potential-energy surface is shown in Fig. 1(a). Our results show a single energy minimum. This minimum corresponds to an adsorption position [point (m1) in Fig. 1(a)] where the Ga adatom forms a bond with the N surface atom. The corresponding bond length is 2.09 Å which is by ≈5% elongated with respect to the bond length in bulk GaN. The binding energy is 2.17 eV.[17] The energetically lowest transition site for diffusion along the *a* direction is exactly at the midst of two N surface atoms [point (t2) in Fig. 1(a)] and the corresponding barrier is $\Delta E_{\perp[0001]}^{m\text{-plane}}=0.21$ eV. In contrast, the energetically lowest transition site for diffusion along the *c* direction is found to be exactly at the midst of two Ga surface atoms [point (t1) in Fig. 1(a)]. The corresponding barrier is significantly larger ($\Delta E_{\parallel[0001]}^{m\text{-plane}}=0.93$ eV) than the one for diffusion along the *a* axis.

A striking result of our calculations is the large anisotropy in the diffusion barriers along and perpendicular to the *c* axis. In order to understand the origin of the large anisotropy in the diffusion barriers we plot the valence charge density for selected lateral positions of a Ga adatom along the low and high diffusion barrier paths. We chose four lateral posi-

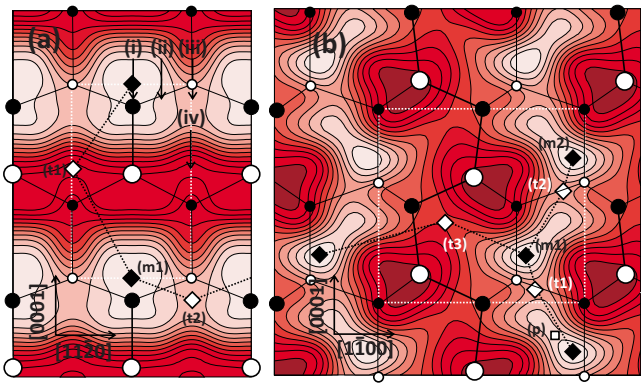

FIG. 1. (Color online) Contour plot of the PES for Ga adatom diffusion on the (a) *m*-plane and (b) *a*-plane surfaces. White large (small) balls correspond to first (second) layer Ga atoms and black large (small) balls to first (second) layer N atoms. The black diamonds (denoted by m1 and m2) represent minima and white diamonds (denoted by t1, t2, and t3) represent saddle points of the PES. The white rectangles denote the corresponding 1×1 surface unit cells. The arrows denoted by (i)–(iv) show the lateral positions of the Ga adatom shown in Fig. 2(i)–(iv), respectively. Each contour line in both plots represents an energy step of 0.1 eV. Cold/lighter (hot/darker) colors correspond to smaller (larger) energy values.

tions for the Ga adatom: on top of a N surface atom [point (i) in Fig. 1(a)], and at the transition sites for diffusion along the *a* and *c* directions [points (iii) and (iv) in Fig. 1(a), respectively]. The corresponding plots are shown in Fig. 2. At the first position which is close to the minimum of the PES the Ga adatom forms a single strong bond with the nearest N surface atom. In order to move the Ga adatom over to the neighboring adsorption site this bond has to be broken. As the adatom moves toward the next minimum (along the [11$\bar{2}$0] direction) the system is initially able to conserve the bond length [Fig. 2(ii)]. However, when the Ga adatom is at the transition site [Fig. 2(iii)] it is no longer able to keep the ideal bond length. The bond is stretched by ≈16% which indicates a significant reduction in bond strength. This reduction in the original bond is to a large extent compensated by the formation of a second bond. This bond is equivalent to the original one and belongs to the next minimum the adatom is jumping into. We can therefore state that the origin of the low diffusion barrier along the *a* axis is the rather small

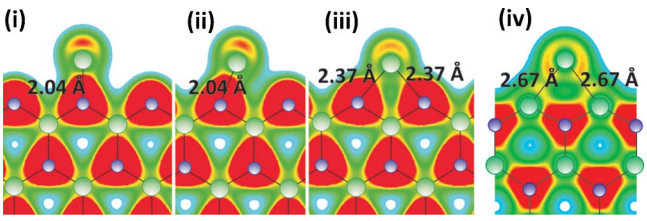

FIG. 2. (Color online) Cross-sectional view of the valence charge density for selected points of the low-energy diffusion path of a Ga adatom on the *m*-plane. The corresponding lateral positions [(i)–(iv)] are indicated by the four arrows in Fig. 1(a). Large (small) balls denote Ga (N) atoms. Hot/dark colors represent larger charge-density values.

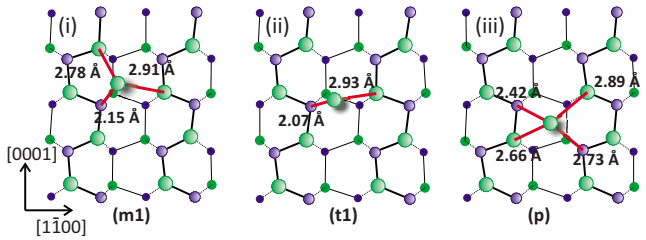

FIG. 3. (Color online) Schematic (top) view of a Ga adatom at three selected lateral positions along the low barrier diffusion path on the *a*-plane surface: (i) at the minimum of the PES [point (m1) in Fig. 1(b)], (ii) at the transition point [point (t1) in Fig. 1(b)], and (iii) at the shallow valley of the next PES minimum [point (p) in Fig. 1(b)]. Green/light (blue/dark) balls denote Ga (N) atoms.

separation distance of two neighboring N surface atoms (≈3.25 Å), which allows the Ga adatom to form the new Ga-N bond before the original one is broken. In contrast to the diffusion along [11$\bar{2}$0], the distance between two minima along the [0001] direction is as large as ≈5.29 Å. In order to move the Ga adatom along this direction the strong covalent cation-anion bond has to be broken and be replaced at the transition point [point (t1) in Fig. 1(a)] by two rather weak metallic Ga-Ga bonds (bond length 2.67 Å). The corresponding charge-density plot is shown in Fig. 2(iv). As a consequence of the unfavorable barrier geometry, the Ga adatom exhibits a substantially larger energy barrier for diffusion along the *c* direction.

Next we focus on the diffusion of a Ga adatom on the *a*-plane surface. We use 35 inequivalent lateral positions in order to sample the potential-energy surface which is shown in Fig. 1(b). Our results show two minima which are denoted as (m1) and (m2) in Fig. 1(b). Both are located close to the two N surface atoms. The corresponding Ga-N bond length is 2.15 Å which is slightly larger (≈8%) compared to the corresponding bond length in bulk GaN (1.98 Å). In addition to the bulklike bonds, it forms two bonds with neighboring surface Ga atoms. The corresponding bond lengths 2.78 and 2.91 Å are close to the nearest-neighbor distance in bulk *α*-Ga [2.79 Å,[18] see also Fig. 3(i)]. The binding energy of the Ga adatom at this site is 2.30 eV.[17] To move to a neighboring minimum three barrier configurations (transition points) denoted as (t1), (t2), and (t3) exist: (t1) and (t2) are symmetry equivalent and correspond to the diffusion barriers when going along the *c* axis (i.e., along the Ga-N dimer chains), while (t3) is the barrier for crossing one of the chains, i.e., for moving along the *m* axis. Our calculations reveal a strong anisotropy for diffusion along and perpendicular to the Ga-N dimer chains: The diffusion barrier along the *c* axis is $\Delta E^{a\text{-plane}}_{\parallel[0001]}=0.32$ eV, while for diffusion perpendicular to it, it is almost two times larger: $\Delta E^{a\text{-plane}}_{\perp[0001]}=0.63$ eV. The diffusion along the low barrier path on the *a*-plane surface is schematically shown in Fig. 3: The diffusion can be viewed as a zigzag jump of the Ga adatom between two adjacent Ga-N dimer chains. The fact that the Ga adatom is able to form alternating bonds explains the low diffusion barrier along this path.

The anisotropy in the kinetic parameters of the Ga adatoms may be attributed to the specific geometry and stoichi-

TABLE I. Ga adatom diffusion barriers E_{diff} on *a*- and *m*-plane Ga-N dimer surfaces for migration paths parallel and normal to the *c* axis and the corresponding axial over lateral diffusion length ratios for 1000, 1150, and 1400 K, characteristic of molecular beam epitaxy (MBE) growth of GaN, of NWs, and hydride vapor phase epitaxy (HVPE) growth of GaN films, respectively.

			$L^{\mathrm{axial}}/L^{\mathrm{lateral}}$		
Surface	$\parallel$ to [0001] (eV)	$\perp$ to [0001] (eV)	1000 K	1150 K	1400 K
a-plane	0.32	0.63	6.042	4.778	3.614
m-plane	0.93	0.21	0.015	0.026	0.051

ometry of the nonpolar GaN surfaces: These surfaces consist of two chemically very different species which exhibit different bonding properties in terms of enthalpies and lengths with the Ga adatoms, i.e., weak metallic Ga-Ga bonds versus strong covalent Ga-N bonds. Moreover, due to the specific symmetry of the nonpolar surfaces and the relatively small lattice constant of GaN, kinetic pathways are realized which allow the Ga adatoms to efficiently compensate for the strong covalent bonds they form at the PES minima. These geometry driven directions correspond to the low diffusion barrier pathways. Therefore the low diffusion barrier path on the *m*-plane (*a*-plane) surface is normal (parallel) to the *c* direction where the separation distance between two neighboring adsorption sites is ≈ 3.25 Å (≈ 3.23 Å), respectively. We note, that in contrast for the high barrier diffusion paths the separation distances are ≈ 5.29 Å and ≈ 5.63 Å for *m* and *a* planes, respectively. The migration barriers for both nonpolar surfaces are summarized in Table I. We note that the Ga adatom kinetics on the nonpolar surfaces are qualitatively different to that on polar GaN surfaces.[19] Polar surfaces are strongly Ga stabilized, and the adatom surface interaction is dominated by delocalized metallic Ga-Ga bonds: as a consequence the diffusion barriers are low and isotropic with values of ≈ 0.4 eV and ≈ 0.2 eV for the (0001) and $(000\bar{1})$ surface, respectively.

Finally, we studied the diffusion of a N adatom on these surfaces. Our results show for this case qualitatively different adatom kinetics: placing a N adatom close to a surface N atom, it attracts the N surface atom, forms a strong N-N bond, and desorbs together with a surface N atom as a N molecule. This hitherto not reported behavior has been found for both *a*- and *m*-plane surfaces. We therefore conclude that both nonpolar and stoichiometric surfaces are unstable against atomic N. Moreover, this finding clearly indicates that the diffusion anisotropy on the nonpolar surfaces can be attributed solely to Ga adatoms: they thus constitute the rate limiting factor in adatom kinetics. This is in clear contrast to the adatom kinetics on the polar GaN surfaces where calculations by Zywietz *et al.*[19] revealed that N-rich surface morphologies can be kinetically stabilized on the polar GaN surfaces and that N adatoms diffuse significantly slower than Ga adatoms and are therefore the rate limiting factor.

The calculated strong in-plane anisotropy of the Ga adatom kinetics is an inherent and universal characteristic of the atomic geometry and chemistry of stoichiometric nonpolar GaN surfaces. It is also in accordance with the experimentally observed slatelike morphology on nonpolar surfaces. Although also other mechanisms such as surface preparation, off-axis substrates, and/or the presence of stacking faults may cause surface anisotropy, we note that the fast diffusion directions agree with the experimentally observed orientation of the slates. Recent experimental reports also provide strong evidence that the in-plane growth anisotropy is reduced by increasing the growth temperature.[20] This observation is consistent with our data (Table I): with increasing temperature the anisotropy in the diffusion lengths decreases. It also explains the *m*-plane GaN quantum dot to quantum wire transition reported recently by Amstatt *el al.*[21]

Recent experiments provide evidences that the side facets of the *c*-axis GaN NWs consist of *m*-plane surfaces.[22,23] This is consistent with previous[11] and our present results that the *m* plane has a ≈ 5 meV/Å^2 lower surface energy than the *a* plane. Based on the corresponding diffusion barriers a qualitative analysis on the anisotropy of the Ga adatom diffusion lengths can be drawn. The diffusion length L_{diff} for an adatom is proportional to $\sim\sqrt{\Gamma\tau}$, where τ is the average adatom life time, e.g., the time between the events of adatom adsorption and adatom incorporation or desorption. Γ is the diffusion coefficient which is proportional to $\sim\exp(-E_{\mathrm{diff}}/k_BT)$, where E_{diff} is the diffusion barrier and k_B and T are the Boltzmann constant and temperature, respectively. Assuming typical growth temperatures of 1000 K we find that for the diffusion of the Ga adatoms on *m*-plane side facets the axial diffusion length is by 2 orders of magnitude smaller than the lateral one (see Table I). On the other hand the axial diffusion length on the *a*-plane side facets is by 1 order of magnitude larger than the lateral one. Thus, the diffusion induced mechanism, which describes the growth of a NW by material transfer from the side facets to the top, will be less pronounced on *m*-plane side facets. An interesting conclusion of these results is that only Ga adatoms adsorbing in close proximity to the top of the NW are able to reach the top before getting desorbed or incorporated into the side facets. Therefore only a small fraction of Ga adatoms reaching the wire contribute to axial growth. Alternatively at the edges of the NW *a*-plane facets may form which provide much faster diffusion to the top. This conclusion is consistent with experimental observations on MBE grown GaN NWs: Based on SEM micrographs the adatom diffusion length on the NW side facets was estimated to be less than 100 nm.[24]

Our calculations further revealed that stoichiometric nonpolar GaN surfaces, which are thermodynamically stable for a wide range (moderate to N rich) of N chemical potentials,[14] are intrinsically unstable against atomic N. Since it is not clear whether the active N in, e.g., a plasma-assisted MBE chamber corresponds to atomic N, charged N, or excited molecular N, further experiments are required in order to elucidate the role of N on the growth kinetics of the nonpolar GaN surfaces. N-rich surface configurations or reconstructions are thermodynamically highly unfavorable even for extreme N-rich growth conditions. This is in contrast to the *c*-plane GaN surfaces where N adatoms can be either thermodynamically stabilized in the form of a 2×2 N adatom reconstruction for extreme N rich conditions[25] or kinetically due to the huge N adatom diffusion barriers.[19] Therefore,

island nucleation and Ga adatom incorporation events are expected to be more probable and frequent on the *c*-plane surface which forms the top of the NW. The higher nucleation rate at the top is expected to promote the axial over radial growth of the NWs. A consequence of this finding is that the NW diameter should be preserved during growth. This has indeed been observed experimentally by Ristić *et al.*[26] A counterintuitive consequence of this mechanism is that under N-rich conditions N adatoms will be the limiting factor for island nucleation.

In summary, we have investigated adatom kinetics on *a*- and *m*-plane GaN surfaces using density-functional theory. We have found a strong in-plane anisotropy of the diffusion barriers for both surfaces: on the *a*- (*m*-)plane surface Ga adatoms exhibit substantially smaller (larger) diffusion barriers along the *c* axis. These findings have interesting consequences on the growth of GaN NWs oriented along the *c* axis: the larger axial over lower radial growth rates cannot be attributed only to the diffusion-induced mechanism. Rather the *c*-oriented NW growth is promoted by the larger nucleation and incorporation rates on the top NW surface with respect to the corresponding rates on the side facets.

We acknowledge financial support by the German Research Foundation (Research Group FOR 506) and EU RTN PARSEM. L.L. would like to thank H. A.-Farsakh for his valuable help on the PW interpolation scheme.

*lymperakis@mpie.de

[1] P. Waltereit, O. Brandt, A. Trampert, H. T. Grahn, J. Menniger, M. Ramsteiner, M. Reiche, and K. H. Ploog, Nature (London) **406**, 865 (2000).

[2] H. Wang, C. Chen, Z. Gong, J. Zhang, M. G. M. Su, J. Yang, and M. A. Khan, Appl. Phys. Lett. **84**, 499 (2004).

[3] P. Waltereit, O. Brandt, M. Ramsteiner, R. Uecker, P. Reiche, and K. H. Ploog, J. Cryst. Growth **218**, 143 (2000).

[4] C. Q. Chen *et al.*, Appl. Phys. Lett. **81**, 3194 (2002).

[5] T. Paskova, V. Darakchieva, P. Paskov, J. Birch, E. Valcheva, P. O. A. Perssona, B. Arnaudov, S. Tungasmitta, and B. Monemar, J. Cryst. Growth **281**, 55 (2005).

[6] K. Kusakabe and K. Ohkawa, Jpn. J. Appl. Phys., Part 1 **44**, 7931 (2005).

[7] D. S. Li, H. Chen, H. B. Yu, X. H. Zheng, Q. Huang, and J. M. Zhou, J. Cryst. Growth **265**, 107 (2004).

[8] Y. J. Sun, O. Brandt, and K. H. Ploog, J. Vac. Sci. Technol. B **21**, 1350 (2003).

[9] J. C. Johnson, H. J. Choi, K. P. Knutsen, R. D. Schaller, P. D. Yang, and R. J. Saykally, Nature Mater. **1**, 106 (2002).

[10] L. Geelhaar, C. Chze, W. M. Weber, R. Averbeck, H. Riechert, T. Kehagias, P. Komninou, G. P. Dimitrakopulos, and T. Karakostas, Appl. Phys. Lett. **91**, 093113 (2007).

[11] J. E. Northrup and J. Neugebauer, Phys. Rev. B **53**, R10477 (1996).

[12] U. Grossner, J. Furthmüller, and F. Bechstedt, Phys. Rev. B **58**, R1722 (1998).

[13] C. D. Lee, R. M. Feenstra, J. E. Northrup, L. Lymperakis, and J. Neugebauer, Appl. Phys. Lett. **82**, 1793 (2003).

[14] D. Segev and C. G. V. de Walle, Surf. Sci. **601**, L15 (2007).

[15] G. Kresse and J. Hafner, Phys. Rev. B **47**, 558 (1993).

[16] G. Kresse and J. Furthmüller, Phys. Rev. B **54**, 11169 (1996).

[17] The Ga adatom binding energy is defined as $E^{\mathrm{bind}}=-(E_{\mathrm{tot}}^{\mathrm{adatom}}-E_{\mathrm{tot}}^{\mathrm{slab}}-E_{\mathrm{tot}}^{\mathrm{atom}})$, where $E_{\mathrm{tot}}^{\mathrm{adatom}}$, $E_{\mathrm{tot}}^{\mathrm{slab}}$, and $E_{\mathrm{tot}}^{\mathrm{atom}}$ are the total energy of the slab with the adatom, the slab, and the free spin-polarized Ga atom, respectively.

[18] M. Bernasconi, G. L. Chiarotti, and E. Tosatti, Phys. Rev. B **52**, 9988 (1995).

[19] T. Zywietz, J. Neugebauer, and M. Scheffler, Appl. Phys. Lett. **73**, 487 (1998).

[20] A. Hirai, B. A. Haskell, M. B. McLaurin, F. Wu, M. C. Schmidt, K. C. Kim, T. J. Baker, S. P. DenBaars, S. Nakamura, and J. S. Speck, Appl. Phys. Lett. **90**, 121119 (2007).

[21] B. Amstatt, J. Renard, C. Bougerol, E. Bellet-Amalric, B. Gayral, and B. Daudin, Phys. Rev. B **79**, 035313 (2009).

[22] K. A. Bertness, A. Roshko, L. M. Mansfield, T. Harvey, and N. Sanford, J. Cryst. Growth **300**, 94 (2007).

[23] L. Largeau, D. L. Dheeraj, M. Tchernycheva, G. E. Cirlin, and J. Harmand, Nanotechnology **19**, 155704 (2008).

[24] R. K. Debnath, R. Meijers, T. Richter, T. Stoica, R. Calarco, and H. Loth, Appl. Phys. Lett. **90**, 123117 (2007).

[25] J. E. Northrup, J. Neugebauer, R. M. Feenstra, and A. R. Smith, Phys. Rev. B **61**, 9932 (2000).

[26] J. Ristic, E. Calleja, S. Fernandez-Garrido, L. Cerutti, A. Trampert, U. Jahn, and K. H. Ploog, J. Cryst. Growth **310**, 4035 (2008).